Results in Physics 7 (2017) 3287–3300

Contents lists available at ScienceDirect

Results in Physics

journal homepage: www.journals.elsevier.com/results-in-physics

Absolute variation of the mechanical characteristics of halloysite reinforced polyurethane nanocomposites complemented by Taguchi and ANOVA approaches

Tayser Sumer Gaaz [a,b,*], Abu Bakar Sulong [a,*], Abdul Amir H. Kadhum [c], Mohamed H. Nassir [d], Ahmed A. Al-Amiery [e]

[a] Department of Mechanical & Materials Engineering, Faculty of Engineering & Built Environment, University Kebangsaan Malaysia, Bangi, Selangor 43600, Malaysia
[b] Department of Machinery Equipment Engineering Techniques, Technical College Al-Musaib, Al-Furat Al-Awsat Technical University, Al-Musaib, Babil 51009, Iraq
[c] Department of Chemical & Process Engineering, Faculty of Engineering & Built Environment, Universiti Kebangsaan Malaysia, Bangi, Selangor 43600, Malaysia
[d] Program of Chemical Engineering, Taylor's University-Lakeside Campus, Subang Jaya, Selangor 47500, Malaysia
[e] Energy and Renewable Energies Technology Center, University of Technology, Baghdad, Iraq

ARTICLE INFO

Article history:
Received 24 February 2017
Received in revised form 28 August 2017
Accepted 29 August 2017
Available online 5 September 2017

Keywords:
Nanocomposite
Design-of-experiment
Taguchi optimization method
Mechanical properties

ABSTRACT

The variation of the results of the mechanical properties of halloysite nanotubes (HNTs) reinforced thermoplastic polyurethane (TPU) at different HNTs loadings was implemented as a tool for analysis. The preparation of HNTs-TPU nanocomposites was performed under four controlled parameters of mixing temperature, mixing speed, mixing time, and HNTs loading at three levels each to satisfy Taguchi method orthogonal array L_9 aiming to optimize these parameters for the best measurements of tensile strength, Young's modulus, and tensile strain (known as responses). The maximum variation of the experimental results for each response was determined and analysed based on the optimized results predicted by Taguchi method and ANOVA. It was found that the maximum absolute variations of the three mentioned responses are 69%, 352%, and 126%, respectively. The analysis has shown that the preparation of the optimized tensile strength requires 1 wt.% HNTs loading (excluding 2 wt.% and 3 wt.%), mixing temperature of 190 °C (excluding 200 °C and 210 °C), and mixing speed of 30 rpm (excluding 40 rpm and 50 rpm). In addition, the analysis has determined that the mixing time at 20 min has no effect on the preparation. The mentioned analysis was fortified by ANOVA, images of FESEM, and DSC results. Seemingly, the agglomeration and distribution of HNTs in the nanocomposite play an important role in the process. The outcome of the analysis could be considered as a very important step towards the reliability of Taguchi method.

Introduction

Halloysite nanotubes (HNTs) whose chemical structure is $Al_2Si_2O_5(OH)_4{\cdot}nH_2O$ [1] have been used as nanofillers at certain weight percentage with polymers to enforce the mechanical properties and to enhance physical and thermal properties [2]. The use of HNTs has shown better outcome compared with the traditional nanofillers of carbon nanotubes (CNTs) due to cost and easy processability [3]. Structurally, HNTs are characterized by a variety of geometric sizes ranging between 300–1500 nm in length, 15–100 nm in inner diameter and 40–120 nm in outer diameter [4,5]. Regarding exfoliation, HNTs are not foliated because the layers keep intact; however, HNTs can aggregate or entangled to each other [6]. The crystal structure of HNTs consists of two-layer tetra- and octahedral sheets connected mainly by hydrogen bond. The tetrahedral structure (Si—O—Si) belongs to the external surfaces of the HNTs while the internal surface consists of octahedral (Al—OH) structure. HNTs are characterized by the average pore size of 80–100 Å and aspect ratio of 10–50. The higher the aspect ratio, the better the reinforcing effect [7]. HNTs of 75–82 m^2/g BET surface area and 2.14–2.59 g/cm^3 density outperform other mineral fillers in creating light-weight polymer composite [8].

TPU, discovered in the early 1940s [9], is available with a wide range of hardness [10], ester and ether type, unique physical-

* Corresponding authors at: Department of Mechanical & Materials Engineering, Faculty of Engineering & Built Environment, University Kebangsaan Malaysia, Bangi, Selangor 43600, Malaysia (T.S. Gaaz).
E-mail addresses: taysersumer@gmail.com (T.S. Gaaz), amir@eng.ukm.my (A.A.H. Kadhum), mohamedh.nassir@taylors.edu.my (M.H. Nassir), dr.ahmed1975@gmail.com (A.A. Al-Amiery).

http://dx.doi.org/10.1016/j.rinp.2017.08.066
2211-3797/

chemical properties, and empowered by its versatility, has been strengthening its importance in many applications [11]. TPU mixed with nanofillers of HNTs or CNTs has been under investigation using several techniques. The morphology and surface characterizations were examined by XRD [12–14]. SEM images for the nanocomposites were prepared by Pizzatto et al. [14,15] while TEM was employed by Dan et al. [13]. The characterization of the bonding was carried out by FTIR [13,15]. The thermal properties and surface characterization were performed by TGA and DSC techniques [12,15]. Generally, HNTs possesses important characteristics such as enhanced thermal stability, impeding crack growth, and strengthening the mechanical properties of nanocomposites [16]. In addition, the relatively cheap HNTs shares its counterpart, CNTs, similar characteristics of a longitudinal hollow structure which allows it to form layers of tetrahedral sheets of silica and octahedral sheets of alumina [4,17,18]. For these reasons, the applications of HNTs are extended to include cosmetics reinforcement, catalyst carriers, and drug delivery due to its unusual shape and geometry, surface properties, chemical formation and cost-efficiency [19]. In this paper, HNTs are used to reinforce TPU.

The preparation of HNTs-TPU nanocomposites involves implementing several parameters during mixing process which makes optimization very difficult to achieve. The delicacy of the process is tied to the designing of a number of trials for optimization. Currently, there have been a few attempts to reduce the number of trials without affecting the qualities of experimentation. One of these attempts was statistically formalized by the design of experiment (DOE) in late 1935s [20]. Taguchi proposed such a design for a system of experiments to achieve optimization with a reasonable number of trials. In this regard, Taguchi designing method starts with selecting specific control factors. To achieve this optimization, Taguchi proposed an experimental plan in terms of orthogonal arrays (OAs), which include different combinations of parameters in conjunction with their levels for each trial, suggesting that the entire parameter space could be performed with a minimum number of trials [21,22]. Interaction among factors could be determined and a lesser number of experiments would be needed to get the desired accuracy [23].

There are two approaches for maximizing the controlled parameters: static and dynamics. In static approach, the noise and the controlled parameters are fed together for processing the output [24]. In the dynamic approach, the noise, the controlled parameters, and an external noise are fed together for processing the output. In this current work, the static approach was employed for simplicity. Mixing parameters yields a response which could be determined according to signal-to-noise (S/N or SNR) ratio. Statistically, the noise measurement is conducted according to several schemes [25]. In this work, the scheme chosen is "larger is better" where the response is maximized and the output is positive always according to $S/N = -10\log\sum\frac{1}{y^2}/n$.

The development of new composites of HNTs and TPU through employing an internal mixer requires proper settings for such parameters as mixing temperature, speed, time, and the loading of the HNTs filler with the thermoplastic in order to optimize these parameters to achieve the best results [26,27]. Gholami and Sadeghi [12] studied different clay-TPU nanocomposites via melting the mixture, and their findings showed that these materials have a very close dispersion to exfoliation [12]. In another study, Shokoohi et al. [21] found that the mixing parameters affect the average particle size as, for example, the twin screw extruder produces smaller particles with a more narrow distribution of sizes than the single screw extruder [21]. Accordingly, the number of trials in the current plan, based on Taguchi L_9 orthogonal arrays, has been reduced to only nine [21] out of the 27 trials in the traditionally employed techniques. Traditionally, for instance, a set of three experiments with three trials for each requires 27 trials, which, apparently, is difficult, costly, and time-consuming to conduct in the industry. The Taguchi method of DOE has been used for quite some time to improve products, manufacturing processes and, more specifically, challenging quality problems. The Taguchi method of analysis in conjunction with statistical experimental design has become popular based on the most recent work [28–30] and is a widely used technique for optimization and improving qualities [31]. The outcome of using the Taguchi method is the optimization of the manufacturing process and design [32–34]. In addition to the optimization process employed by Taguchi method, the results have been analysed by ANOVA which carried out according to several authors [35]. The aim of this work is to explore how mixing parameters influence the mechanical properties of HNTs-TPU nanocomposites using the best conditions predicted by utilizing the Taguchi statistical method to obtain the optimum conditions for the best mechanical properties.

Results and discussion

Characterization of neat HNTs

The following characterizations are important for supporting the validity of nano characteristics of HNTs and to show the size of HNTs.

TEM of HNTs

The neat HNTs were investigated using low and high magnification TEM at 100 kV, as shown in Fig. 1(a) and (b), respectively. The basic purpose of the TEM tests was to identify the physical HNTs structure. At a lower magnification, a group of nanotubes appeared at different lengths and diameters, as shown in Fig. 1(a). In order to have a better understanding of accurate dimensions, TEM images were taken at a higher magnification. These images enabled us to measure the dimensions of each nanotube. A typical measurement showed that the inner diameter of the nanotubes was 16.02 nm while the outer diameter was 55.89 nm. These measurements are within the range suggested by other studies of 10–30 nm and 50–100 nm, for inner and outer diameters, respectively. The TEM images also showed that the nanotubes were agglomerated in various groups with various sizes and arbitrary orientations.

FESEM of HNTs

The topography of the surface of the neat HNTs was investigated by FESEM at low and high magnification, as shown in Fig. 2(a) and (b), respectively. FESEM images depict an in-depth-investigation of the HNTs block matrix. The FESEM images of neat HNTs at a lower magnification are shown in Fig. 2(a) and at a higher magnification in Fig. 2(b).

Taguchi analysis of HNTs-TPU nanocomposites

The experimental procedure and the relevant results guided by the Taguchi method is a very powerful approach that offers very delicate and accurate guidance for minimizing the number of experiments and optimizing the performance of the experiment. In the following sections, detailed procedures for the calculation of the mechanical properties of HNTs-TPU nanocomposites are presented.

Taguchi method

The L_9 orthogonal array Taguchi method was carried out at three levels and four controlled parameters as shown in Table 1. The average of S/N ratio which measures the sensitivity of the mechanical properties was determined using Minitab software

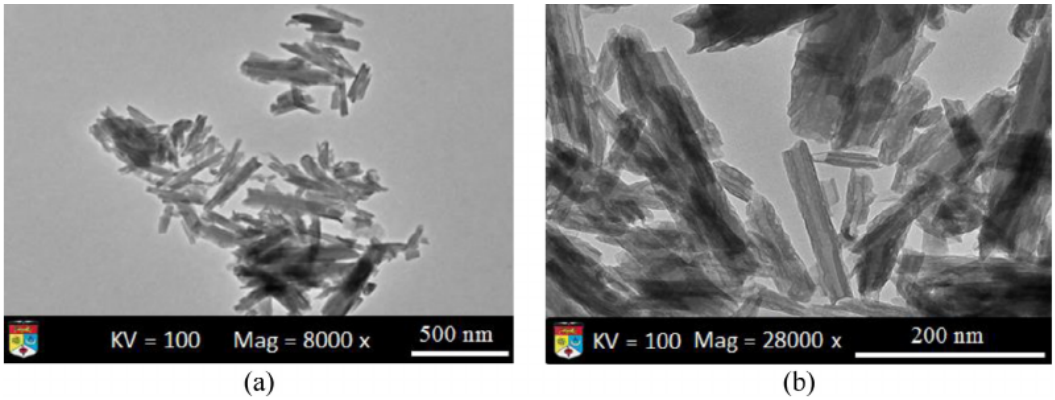

Fig. 1. TEM images of neat HNTs: (a) at 8 k× (low magnification), and (b) 28 k× (high magnification).

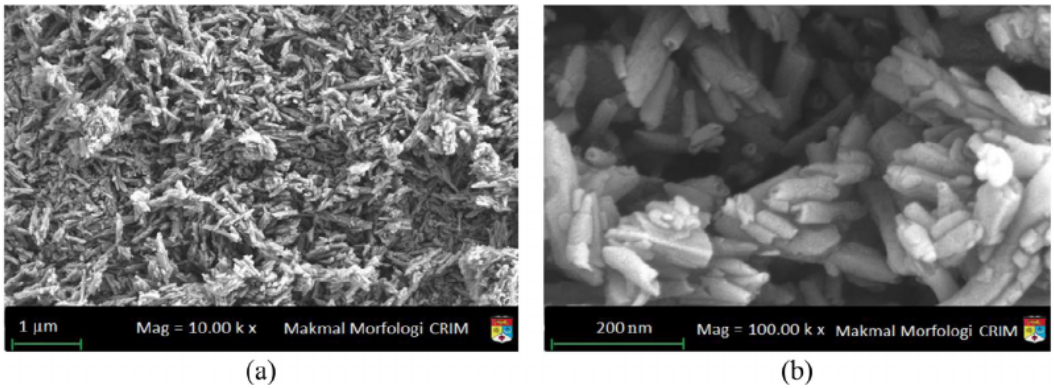

Fig. 2. FESEM microphotographs for neat HNTs (a) low and (b) high magnification.

Table 1
The parameters for three levels of selected factors.

Controlled factors	Level 1	Level 2	Level 3
Mixing temp. (°C)	190	200	210
Mixing speed (rpm)	30	40	50
Mixing time (min)	20	30	40
HNTs loading (wt.%)	1	2	3

(version 16). The noise sensitivity of each response was measured in conjunction with the noise caused by controlled parameters. Based on [36], the higher S/N ratio value is resulted from a small variance of that parameter. The average of S/N was calculated and fully explained in Appendix A.

Selecting the processing parameters

The controlled parameters, their levels, and the response are the essential parts of the Taguchi method. The decision regarding the controlled parameters and the responses is based on the nature of the experiment while the domain of the proposed levels of the controlled parameters depends on the physical properties of the controlled parameters. In this current work, investigating the mechanical properties of the HNTs-TPU nanocomposites was set as a goal due to the need of the enhanced product which includes the tensile strength, Young's modulus, and the tensile strain. These three parameters are enough to determine the applicability of the HNTs-TPU nanocomposites product regarding strength and strain. The preparation of HNTs-TPU nanocomposites requires mixing HNTs at certain wt.%. In order to achieve a homogenous mixture, the mixture has to be mixed at a certain temperature, speed, and time. The HNTs-TPU nanocomposites, mixing temperature, mixing speed, mixing time, and HNTs loading are known as the controlled parameters. The controlled parameters have to be employed at the minimum of two levels depending on preliminary or manufacturer's assessments of the physical properties such as melting temperature, density, exfoliation, and the thermal stability of the mixture components.

The mixing ratio of HNTs and TPU in this work was chosen at three levels of 1, 2, and 3 wt.% HNTs. Previous researchers have chosen the variety of percentages [37]. Based on previous trials, additive of more than 3 wt.% of HNTs has shown that the optimization of the mechanical properties declined instead of showing improvement [38]. Based on previous work [14], loading was performed within wt. ratios of no more 10 wt.% [14]. Regarding mixing temperature, thermal properties of HNTs and TPU have to be considered and, consequently, three levels of 190, 200, and 210 °C were chosen. The temperatures choice is slightly different from the published works of El-Shekeil et al. [26] due to their HNTs-TPU nanocomposites preparation and the origin of TPU. The levels of chosen temperature in [26] is 10 °C lower than the temperature employed in the current work. The third controlled parameter is the speed of the mixing process. Three speeds are selected at 30, 40, and 50 rpm based on the manufacturer recommendation and available information from previous work [26]. El-Shekeil et al. [26] have concluded that low speeds do not produce a homogenous mixture while high speeds may cause breakage of filler. The fourth controlled parameter is the time allowed for mixing process. Three levels for mixing time were chosen at 20, 30, and 40 min based on mere observing the stabilization of the twin screw as an indicator for homogeneous mixture or good dispersion [26]. On the other

hand, the more time subsequent torque stabilization of the mixture, the more thermal degradation and breakage of the mixture would occur [26]. Table 1 contains the controlled factors and their relevant levels.

The total number of trials as suggested by Taguchi method is 9 as shown in Table 2, where all controlled parameters are shown. In the following paragraphs, all results of the controlled parameters are discussed.

Measurements of mechanical properties

HNTs-TPU nanocomposites were tested for mechanical properties. Nine runs were prepared according to the criteria in Tables 1 and 2 and, as such, the tensile strength, Young's modulus, and the tensile strain were measured and tabulated in Table 3. The measurements are based on dividing each of the nine samples into three pieces experimented separately. The results and their counterparts S/N's were calculated according to the criteria of "larger is better" as explained in Appendix A where the average of each experimented response of tensile strength, Young's modulus, and tensile strain was determined. The results of the average of each response and its relevant S/N values are listed in Table 3.

Mechanical data analysis

The maximum variations of the tensile strength are taken from trial 1 (highest) and trial 8 (lowest) as proposed in Table 3 and shown numerically in Table 4. The tensile strength of the TPU matrix is reported in Table 3 at 17.7 MPa. The highest and the lowest values of the tensile strength are recorded at 25.25 MPa and 13.13 MPa at the following sets of the controlled parameters (190 °C, 30 rpm, 20 min, and 1 wt.% HNTs loading) and (210 °C, 40 rpm, 20 min, and 3 wt.% HNTs loading), respectively. The highest and lowest variation of the tensile strength are calculate based on the tensile strength of the neat TPU (17.7 MPa) and the highest and lowest values shown in Table 3. The absolute variation between the highest and lowest values of the tensile strength is 69%. A mere observation at the controlled parameters presented in Table 4, one can find out that the mixing time of 20 min is the only parameter appeared in both tensile strength measurements of the two samples. The change in mixing temperature from 190 to 210 °C, mixing speed from 30 to 40 rpm, and the increase in HNTs loading from 1 to 3 wt.% are apparently behind the 69% variation. A correlation among these three controlled parameters and their variations is not difficult to show mathematically; however, a physical justification of the 69% variation is much important and it needs some measurements and investigation. In principle, any of the three remaining parameters have to be collectively taken into consideration.

The melting temperature of TPU matrix (200 °C as recommended by the manufacturer) was tested experimentally and was found to be in the range of 188 °C and 195 °C. The melting temperature is highly dependent on impurities contained in TPU matrix. The temperature of 210 °C causes TPU slightly over melted which is good for mixing but, adversely, causes a primary degradation of TPU bulk which could affect the thermal properties of TPU [39]. The mixing speed of 40 rpm is more than enough which causes HNTs breakage as suggested by El-Shekeil et al. [26] while the mixing speed of 30 rpm is seemingly perfect to provide a homogeneous mixture. The data shows that HNTs loading of 3 wt.% is not convenient to optimize the tensile strength as thought by common sense. The extra of 2 wt.% HNTs incurs an adverse result on the tensile strength value in addition to extra cost. The effect of extra HNTs loading reduces the melting temperature of TPU as seen directly by measurements and supported by Barick & Tripathy [40] as well. As such, the lower mixing temperature of 190 °C seems better because high HNTs loading could lower the melting temperature suggested by the manufacturer to less than 200 °C.

Tables 5 and 6 show the analysis of the Young's modulus and the tensile strain, respectively. The highest value of Young's modulus (11.45 MPa) shows 402% change based on the neat TPU modulus of 2.30 MPa while the lowest value of HNTs-TPU nanocomposites modulus is 3.45 MPa has shown a change of 50%. The absolute variation between the highest and lowest values is 352%. This variation is apparently caused by the mixing temperature, mixing speed, and HNTs loading as the mixing time remains at the same rate for both HNTs-TPU nanocomposites. Seemingly, the high temperature of 210 °C and high HNTs loading of 3 wt.% affect the plasticity of TPU and made it brittle with high Young's modulus while the lower temperature of 190 °C and HNTs loading of 1 wt.% has kept HNTs-TPU nanocomposites in plastic form.

The last analysis is about the tensile strain shown in Table 6. The results of the tensile strain of the HNTs-TPU nanocomposites show that the highest tensile strain occurs at lower mixing temperature, lower mixing speed, and lower HNTs loading where these parameters are essential for keeping the ductility behaviour of the HNTs-TPU nanocomposites.

S/N ratio analysis

The signal-to-noise ratio (S/N) is widely used in science and engineering to compare the level of the desired signal to the level of background noise and it is expressed in decibel (dB). S/N can be applied to any type of signal and if the ratio is greater than one (dB is greater than zero), the system has more signal than noise. The stress response variation was studied by Taguchi method using S/N ratio for the mechanical properties and listed in Table 7 based on the level of the controlled parameters. The effect of the level was not considered in the calculation. Considering the highest effect of the mixing temperature, mixing speed, mixing time, and HNTs loading, the results show that temperature at level I (190 °C), mixing speed at Level I (30 rpm), mixing time at level II (30 min), and HNTs loading at level I (1 wt.%) are the best parameter to optimize the tensile strength. These results are in agreement with the previous Taguchi analysis where no S/N was taken into consideration. The analysis of the tensile strength shows that

Table 2
Effective combination parameters suggested by Taguchi (L_9).

Trial no.	Mixing temp. (°C)	Mixing speed (rpm)	Mixing time (min)	HNTs loading (wt.%)
1	190	30	20	1
2	190	40	30	2
3	190	50	40	3
4	200	30	30	3
5	200	40	40	1
6	200	50	20	2
7	210	30	40	2
8	210	40	20	3
9	210	50	30	1

Table 3
The results of the mechanical properties.

Experiment no.	Tensile strength (MPa)		Young's modulus (MPa)		Tensile strain (%)	
	Average	S/N	Average	S/N	Average	S/N
Neat TPU	17.70	–	2.30	–	430.30	–
1	25.25	28.04	3.45	10.77	1050.72	60.42
2	19.17	25.65	6.54	16.31	990.46	59.91
3	15.79	23.97	10.53	20.45	608.20	55.68
4	16.79	24.50	10.12	20.10	680.76	56.66
5	19.05	25.60	7.77	17.81	1015.50	60.13
6	17.54	24.88	8.05	18.12	870.13	58.79
7	21.24	26.54	6.05	15.64	1005.93	60.05
8	13.13	22.36	11.54	21.24	508.63	54.12
9	21.13	26.50	5.63	15.01	1030.50	60.26

Table 4
Tensile strength analysis.

Tensile strength (MPa) (neat TPU = 17.7 MPa)					
Parameters	Highest	Change %	Lowest %	Change %	Absolute variation %
	25.25	43	13.13	−26	69
Mixing temperature (°C)	190		210		
Mixing speed (rpm)	30		40		
Mixing time (min)	20		20		
HNTs loading (wt.%)	1		3		

Table 5
Young's modulus analysis.

Young modulus (MPa) (neat TPU = 2.30 MPa)					
Parameters	Highest	Change %	Lowest %	Change %	Absolute variation %
	11.54	402	3.45	50	352
Mixing temperature (°C)	210		190		
Mixing speed (rpm)	40		30		
Mixing time (min)	20		20		
HNTs loading (wt.%)	3		1		

Table 6
Tensile strain analysis.

Tensile strain (%) (neat TPU = 430.30%)					
Parameters	Highest	Change %	Lowest %	Change %	Absolute variation %
	1050.72	144	508.63	18	126
Mixing temperature (°C)	190		210		
Mixing peed (rpm)	30		40		
Mixing time (min)	20		20		
HNTs loading (wt.%)	1		3		

Table 7
Average S/N ratio values for tensile properties.

Parameter		Mixing temp. (°C)	Mixing speed (rpm)	Mixing time (min)	HNTs loading (wt.%)
Tensile strength (MPa)	Level I	25.89	26.37	25.10	26.72
	Level II	25.00	24.54	25.55	25.70
	Level III	25.14	25.12	25.37	23.61
Young's modulus (MPa)	Level I	15.85	15.51	16.71	14.54
	Level II	18.68	18.46	17.15	16.69
	Level III	17.30	17.87	17.97	20.60
Tensile strain (%)	Level I	58.68	59.05	57.78	60.27
	Level II	58.53	58.06	58.95	59.59
	Level III	58.15	58.24	58.62	55.49

the same sequence of the parameters as shown in Table 7 are the best for optimization. In other agreement with the previous analysis, Young modulus optimization was taking place at same parameters as shown in Tables 7 and 5. The above analysis shows clearly that the optimization predicted by Taguchi method was accurate and reliable.

ANOVA analysis of mechanical properties

The results analysed by Taguchi method show how each of the three responses under investigation is influenced by a certain controlled parameter or at any given individual level. The analysis is not comprehensive due to the fact that the highest (the lowest) values could take place with some controversy. In order to remove

Table 8
ANOVA average on tensile properties.

	Parameter	Mixing temp. (°C)	Mixing speed (rpm)	Mixing time (min)	HNTs loading (wt.%)	Error %
Tensile strength (MPa)	SS	24.3	76.60	0.81	198.26	29.51
	DF	2	2	2	2	–
	MS = SS/DF	12.1	38.30	0.40	99.13	1.63
	F ratio	7.4	23.36	0.24	60.45	1
	%contribution	6.3	22.25	−0.74	59.16	12.93
Young's modulus (MPa)	SS	14.6	20.89	2.18	127.68	22.01
	DF	2	2	2	2	–
	MS = SS/DF	7.3	10.44	1.09	63.84	1.22
	F ratio	6.0	8.53	0.89	52.19	1
	%contribution	6.5	9.83	−0.13	66.80	16.96
Tensile strain (%)	SS	6075.6	33979.96	39789.68	961112.51	11333.88
	DF	2	2	2	2	–
	MS = SS/DF	3037.8	16989.98	19894.84	480556.25	629.66
	F ratio	4.8	26.98	31.59	763.19	1
	%contribution	0.4	3.10	3.66	91.21	1.55

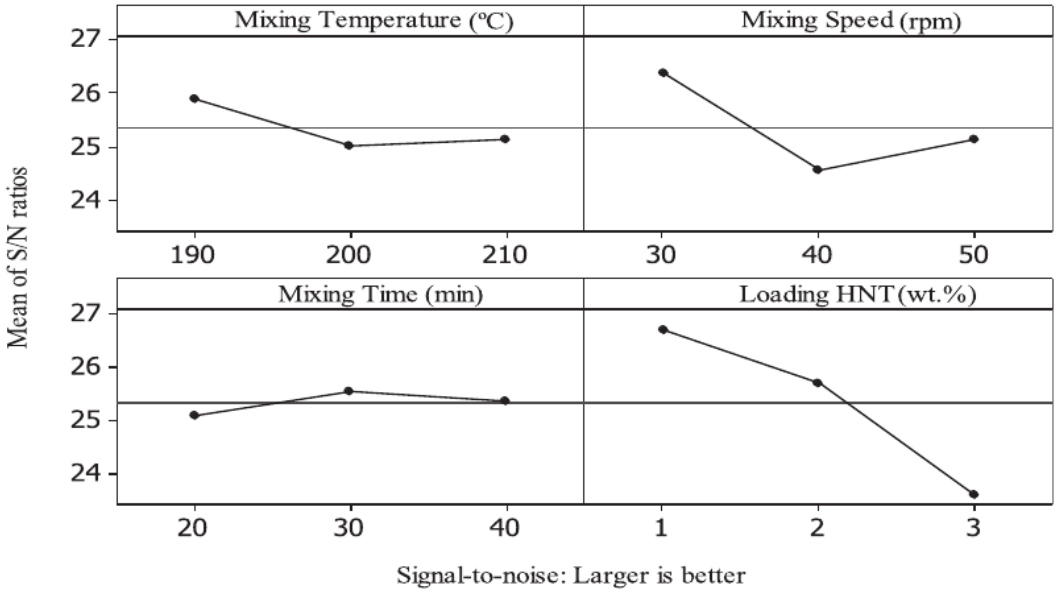

Fig. 3. Main effects plot for S/N ratios on the tensile strength parameter.

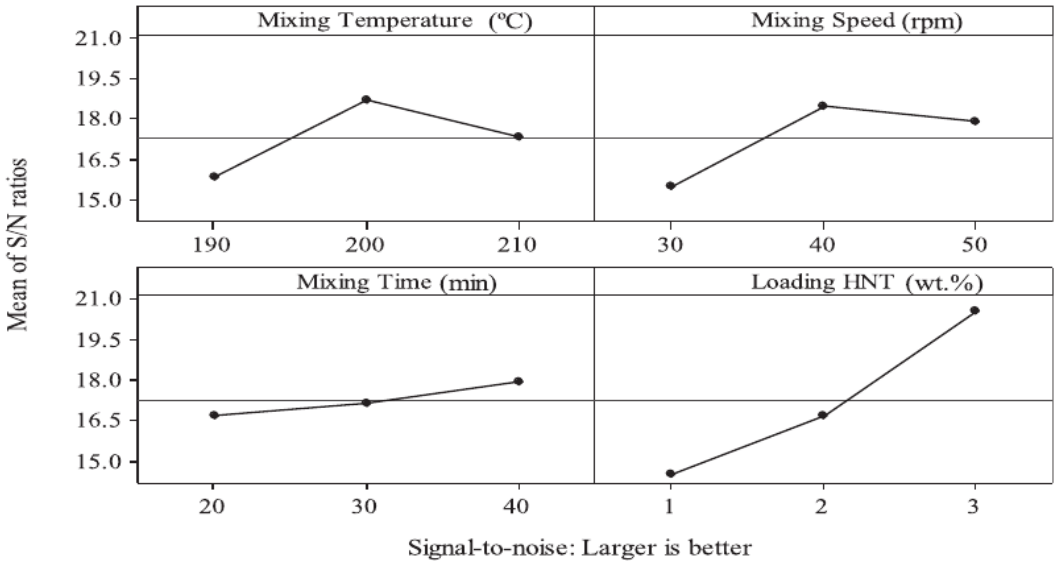

Fig. 4. Main effects plot for S/N ratios on the Young's modulus parameter.

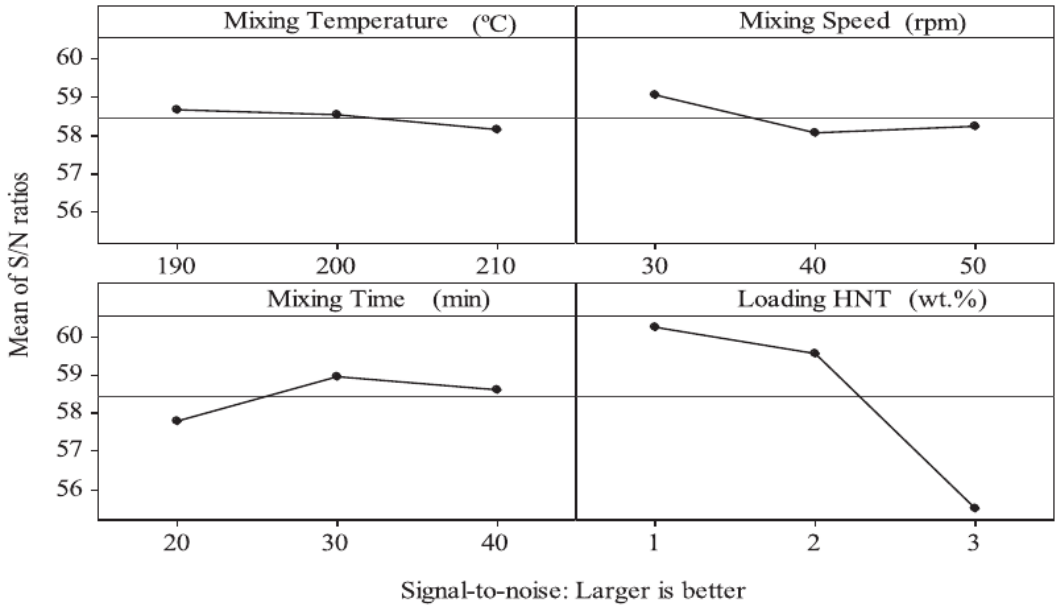

Fig. 5. Main effects plot for S/N ratios on the tensile strain parameter.

these controversial results, if any, ANOVA was employed for further characterization. In ANOVA, the average of all responses is evaluated versus each controlled parameter to have a proper conclusion. ANOVA provides a very powerful approach which suggests whether each controlled parameter is significant or not and, additionally, predicts its level of significance. The data in Table 8 were analysed using ANOVA in order to determine the F-ratio and the percentage contribution of each parameter among other factors. The results of the sum of square (SS), the degree of freedom (DF), mean sum of the square (MS), F ratio for each factor (F-ratio), and the percentage contribution (%contribution) are also listed in Table 8.

The analysis of the data in Table 8 was carried out at 5% significant which means 95% confidence. In this analysis, the focus is about the contribution of each factor which indicates the influence on the results. For tensile strength, the highest contribution comes from loading, followed by mixing speed and then mixing temperature. The contribution of mixing time has a negative effect and can be ignored for its low value as shown in Table 8. The tensile strength is affected mainly by loading whereby the F-ratio is the highest (60%). This result is in a good agreement with the other results despite the fact that the improvement is about 40% for HNTs loading up to 2 wt.% as experimented by Russo et al. [41] and 64% for nanoclay loaded with 3 wt.% as performed by Pizzatto et al. [14]. The significance, measured by the F-ratio, of each factor of mixing temperature, mixing speed, mixing time and loading have a value of 2 wt.% or above which is in agreement with the other results [26]. ANOVA results in Table 8 show that the mixing temperature has a contribution of about 6%, which is very small compared to the loading effect. This is in conflict with the findings proposed by El-Shekeil et al. [42]. The work performed by El-Shekeil et al. [42] is different as the filler was kenaf-bast-fibre, which is very different from the HNTs used in this work. Kenaf-bast-fibre is considered a temperature resistive material and the loading does not show a potential tendency to be an important factor.

It is very important to note that the response measurements are based on "Larger is Better" criteria to evaluate S/N ratios for each controlled parameters. The results are graphically shown for tensile strength, Young's modulus, and tensile strain in Figs. 3, 4, and 5, respectively. The graphical representation of the results shows the highest, the lowest and the middle effect of each level of the controlled parameters on the response. The choice of these effects is concluded by the software rather than direct observations.

Fractured surfaces of optimum tensile specimen

Four samples were chosen for close investigation by FESEM. The first sample is the TPU matrix which was taken as a standard. The second sample was prepared according to the parameters predicted by Taguchi for the highest tensile strength, namely; 190 °C, 30 rpm, 30 min, and 1 wt.% HNTs loading. The other two samples were taken arbitrary at 1 wt.% HNTs-TPU nanocomposites and 3 wt.% HNTs-TPU nanocomposites based on the lowest and highest HNTs loading, respectively. The surface at the fracture of each sample was examined at two magnifications, 1 k× and 5 k×. FESEM is a very useful technique for explaining two features that are related to HNTs loading. The first feature is to show the existence of HNTs in the TPU and the second feature is to show how well HNTs is distributed. TPU matrix was examined first as a reference to demonstrate the fractured surface as shown in Fig. 6(a) at magnifications of 1 k× and 5 k×, respectively. The surface of TPU does not show any irregularities and the presence of hole-like spots is very normal in plastic materials as noted by Barick and Tripathy [43]. The 1 wt.% HNTs-TPU nanocomposites fractured surface is shown in Fig. 6(b) at magnifications of 1 k× and 5 k×, respectively. The fractured surface at the lower magnification clearly shows the presence of HNTs and its distribution. The image at a higher magnification shows agglomeration of HNTs at certain positions on the surface; however, the distribution still looks normal based on the assessment of [14]. For the 3 wt.% HNTs-TPU nanocomposites at 1 k× magnification shown in Fig. 6(c-i) shows the presence of more filler in the fractured surface as expected. The image at a higher magnification of 5 k× shown in Fig. 6(c-ii) shows bigger area of agglomeration of HNTs. The FESEM images of the last sample which was prepared at the optimizing parameters are shown in Fig. 6(d) at a magnification of 1 k× and 5 k×,

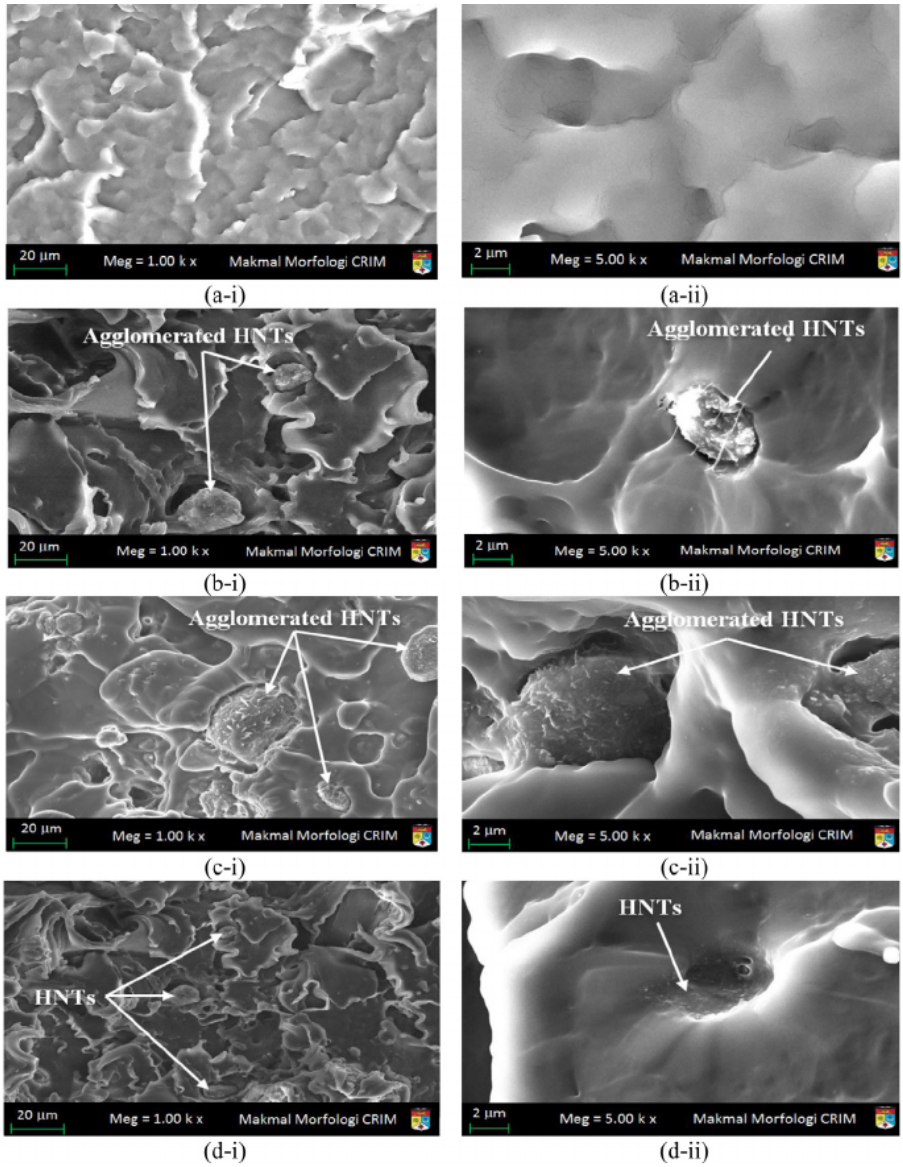

Fig. 6. FESEM (a) TPU matrix, (b) 1 wt.% HNTs-TPU nanocomposites, (c) 3 wt.% HNTs-TPU nanocomposites and (d) optimum parameters of (i) lower magnification of 1.00 k× and (ii) higher magnification of 5.00 k×.

respectively. The surface looks smoother, the filler is very well distributed, and agglomeration appears at very limited spots.

FESEM-fracture surface is another mechanism for analysis. The shape of the fractured surface could be used as indicative to show to a certain certainty whether the sample is purely plastic (imprecise cut) or brittle (precise cut). For TPU, the fractured surface had shown in Fig. 6(a) exhibit imprecise surface reflecting the purely plastic properties of TPU. For the sample of 1 wt.% HNTs-TPU nanocomposites shown in Fig. 6(b), the surface shows agglomeration and slightly sharp cut reflecting the effect of HNTs. The agglomeration of HNTs becomes very clear for the 3 wt.% HNTs-TPU nanocomposites as depicted in Fig. 6(c). As the agglomeration increases, the tensile strength decreases due to the effect of high HNTs content which makes the sample more brittle and easy to break down. The optimized sample shown in Fig. 6(d), the surface is smooth and the agglomeration of HNTs is highly reduced. The results of FESEM are in good agreement with the analysis performed according to Taguchi and ANOVA.

Thermogravimetric analysis of the optimum tensile specimen

The Thermogravimetric analysis (TGA) which shows the percentage weight loss of TPU matrix and HNTs-TPU nanocomposites are shown in Fig. 7(a)–(d) and the results are tabulated in Table 9. The TGA-TPU shown in Fig. 7(a) shows that at 295 °C the structure is still stable while the structures of 1 wt.% HNT-TPU nanocomposites, 3 wt.% HNT-TPU nanocomposites were stable until 280 °C and 285 °C, respectively. The results suggest that TPU matrix is more thermally stable than the HNTs-TPU nanocomposites. For the optimized sample shown in Fig. 7(d), the thermal stability is same as the 1 wt.% HNTs-TPU nanocomposites. TPU with HNTs disturbs the thermal stability of the nanocomposites which suggests that the polymer chain can easily move in the structure [44]. The second stage which is characterized by a 41.11% -weight loss occurred between 290 °C and 470 °C. These results are slightly different from [45] due to different composition and optimizing parameters. The weight loss of TPU matrix and HNTs-TPU nanocomposites during the course of the TGA testing was about 84%, compared to

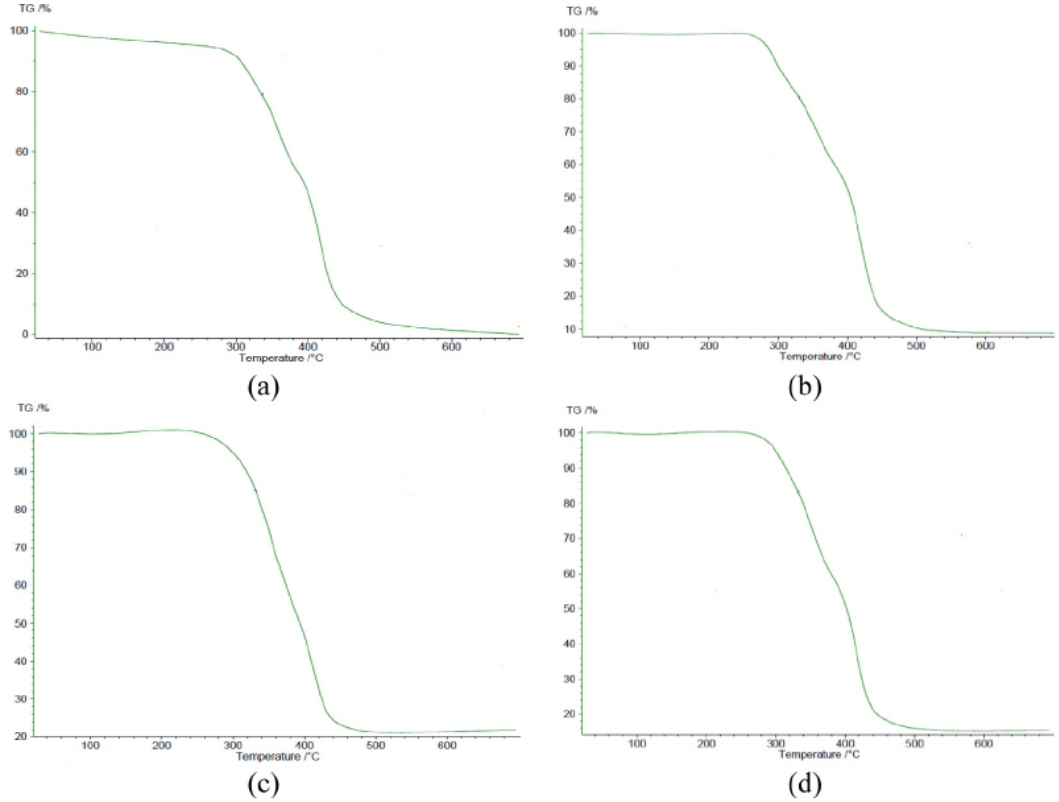

Fig. 7. TGA thermograms of (a) TPU matrix, (b) 1 wt.% HNTs-TPU nanocomposites, (c) 3 wt.% HNTs-TPU nanocomposites, and (d) optimum parameter wt.% HNTs-TPU nanocomposites in a nitrogen atmosphere.

Table 9
TGA results.

Sample	Degradation stage 1		Degradation stage 2		Degradation stage 3	
	T (°C)	Weight loss %	T (°C)	Weight loss %	T (°C)	Weight loss %
TPU matrix	30–295	2.34	295–470	41.11	470–680	8.57
1 wt.% HNT-TPU	30–280	0	280–440	51.21	440–580	12.14
3 wt.% HNT-TPU	30–285	0	285–430	45.45	430–490	20.00
Optimized sample	30–280	0	280–440	52.51	440–490	30.00

about 97% for nanocomposite samples. Seemingly, the loading with HNTs makes the rate of the weight loss faster than the rate of the TPU matrix. In this regard, HNTs loading has a major role in changing the structural and physical properties of the HNTs-TPU nanocomposites, which might be attributed to possible chemical bonding. The accuracy of the HNTs distribution throughout the TPU matrix has another effect on the thermal properties of the HNTs-TPU nanocomposites. It is also suggested that the molecular mobility imparted by the HNTs also plays a vital role in this thermal decomposition phenomenon [46]. The degradation, furthermore, is likely the result of the absorption and adsorption of free radicals generated during the TPU degradation process on the active halloysite particle surface of the nanotubes [12].

Differential scanning calorimetry of the optimum tensile specimen

The differential scanning calorimetry (DSC) is a technique that measures the amount of heat required to increase the temperature of a sample and reference as a function of time or temperature while the reference and the sample are kept nearly at same temperature. As the temperature increases or decreases, phase transition could take place at which more (exothermic) or less (endothermic) heat flows to or out the sample in order to maintain same temperature, respectively. The endothermic phase transition from solid to liquid represents absorption heat by the sample while exothermic process (crystallization) requires less heat to raise the sample temperature. Crystallization is associated with full or partial alignment of the molecular chain which reflects its effect on the mechanical stretching of the polymer depending on the degree of crystallinity. In addition to melting temperature and crystallization temperature, a glass transition is another temperature to be determined by DSC. The glass transition is very important in industrial settings as quality control instrument by showing the purity of the polymer. DSC results are shown in Fig. 8. There are two DSC runs in each result which includes heating (0–300 °C) and cooling (300 °C to 0) where glass transition and melting point are determined in the heating part and crystallization temperature is determined in the cooling stage of the experiment.

The results shown in Fig. 8 are summarized in Table 10. Three stages are recognized: glass transition, melting temperature, and crystallization temperature. The glass temperature is always below the melting temperature because the melting temperature requires more heat to occur. The glass transition occurs at the peak temperature of 102.77 °C for TPU matrix in agreement with [43]. As HNTs loaded to TPU the glass temperature significantly decreased to 69.3 °C and seemingly it did not undergo significant change when the HNTs loaded increased to 3 wt.% nor for the opti-

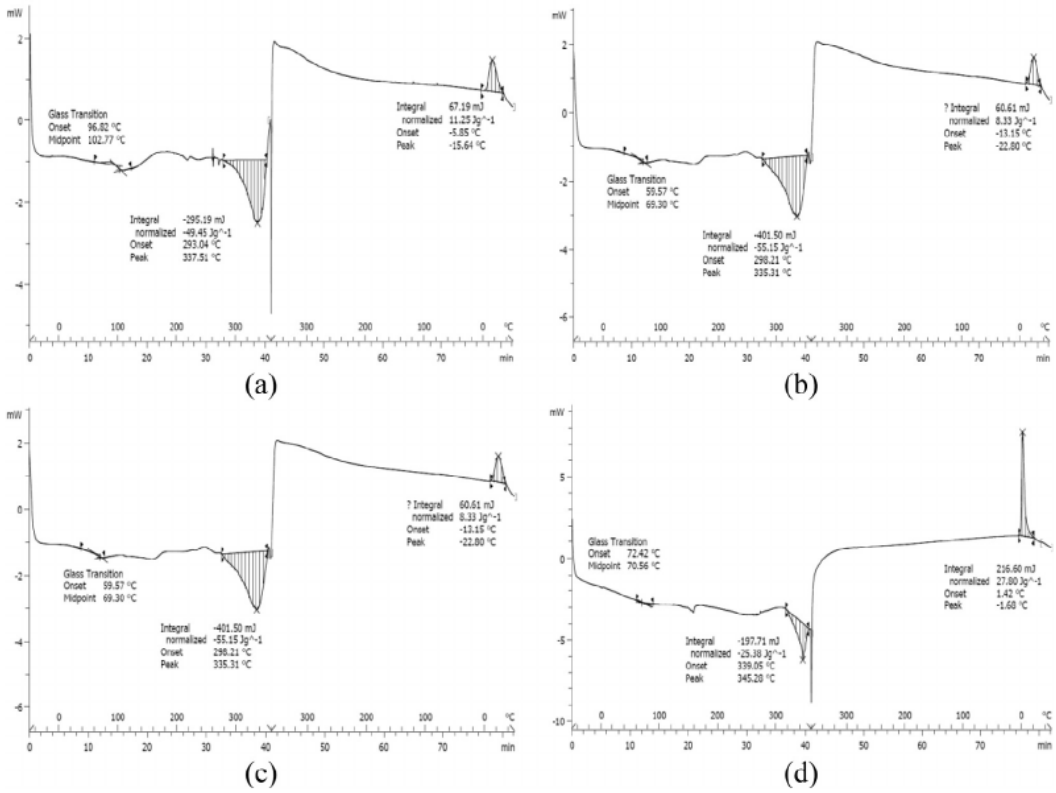

Fig. 8. DSC results (a) TPU matrix, (b) 1 wt.% HNT-TPU nanocomposites, (c) 3 wt.% HNT-TPU nanocomposites, and (d) optimized parameter wt.% HNTs-TPU nanocomposites.

Table 10
DSC results.

Sample	Glass transition temp.			Melting temp.			Crystallization temp.		
	Onset (°C)	Peak (°C)	Integral (mJ)	Onset (°C)	Peak (°C)	Integral (mJ)	Onset (°C)	Peak (°C)	Integral (mJ)
TPU matrix	96.82	102.77	–	293.45	337.51	−295.19	−5.85	−15.64	67.95
1 wt.% HNTs-TPU	59.57	69.30	–	298.21	335.31	−55.15	−13.15	−22.80	60.61
3 wt.% HNTs-TPU	64.76	69.82	–	337.46	343.46	−39.78	−2.47	−8.60	132.06
Optimized sample	72.42	70.56	–	339.05	345.28	−197.71	1.42	−1.68	216.60

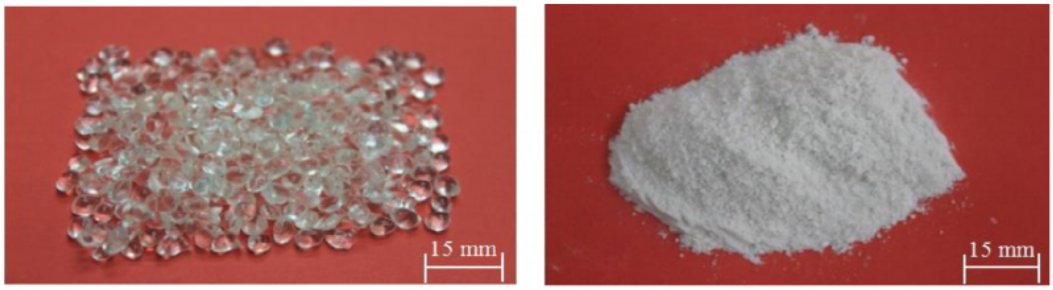

Fig. 9. Manufacturer specifications for (a) TPU matrix of about 5 mm size, and (b) HNTs of 20 nm size.

Table 11
Physical properties of TPU.

Hardness	Tensile strength	Density	Melting temp.	Specific gravity
55D	20 MPa	1224 kg/m^3	200 °C	1.21

Table 12
Chemical composition of HNTs.

Chemical compositions	SiO_2	Al_2O_3	TiO_2	Impurities
Weight %	61.19	18.11	20.11	< 0.5

Table 13
Physical properties of HNTs.

Chemical formula	Surface area (m^2/g)	Pore volume (mL/g)	Density (kg/m^3)	Refractive index
$Al_2Si_2O_5(OH)_4{\cdot}nH_2O$	65	~1.25	2540	1.54

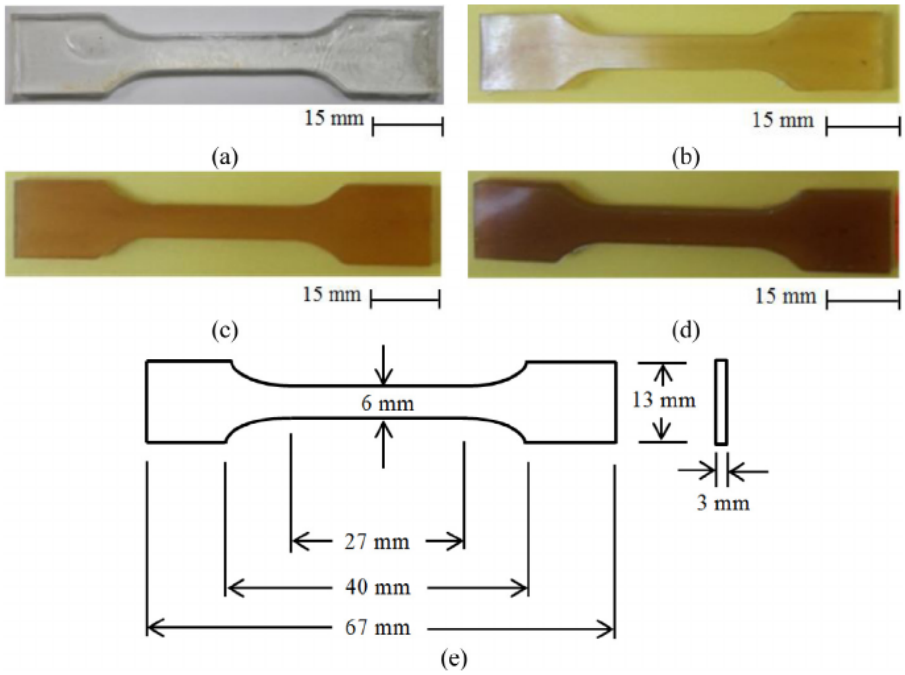

Fig. 10. Samples of HNTs-TPU nanocomposites (a) TPU matrix, (b) 1 wt.% HNTs-TPU nanocomposites, (c) 2 wt.% HNTs-TPU nanocomposites and (d) 3 wt.% HNTs-TPU nanocomposites, and (e) sample dimensions.

mized nanocomposites. The decrease of glass temperature from 102.77 to 69.3 °C exhibits a change from rubber-like state of TPU matrix to brittle glassy state of HNTs-TPU nanocomposites. The melting peak temperature of TPU matrix was recorded by DSC at 337.51 °C which shows no change for 1 wt.% HNTs-TPU nanocomposites and as HNTs loading increased to 3 wt.%, the melting temperature increased to 343.46 °C and remains within a small shift for the optimized HNTs-TPU nanocomposites. The third temperature is the crystallization temperature which appears at −15.64 °C for TPU matrix and shifted to lower temperature of −22.80 °C for 1 wt.% HNT-TPU nanocomposites. The crystallization temperature for 3 wt.% HNTs- is shifted to higher temperature of −8.60 °C and −1.68 °C for the optimized HNTs-TPU nanocomposites. The DSC results support the analysis of mechanical properties by Taguchi and ANOVA as presented earlier as the glass temperature reduced from 96.82 °C to lower temperatures for the composites as shown in Table 10.

Materials and methods

Materials

TPU (Ester type), in the form of semi round shape bead forms of about 5 mm in diameter, was purchased from Global Innovations-polycarbonates Bayer Material Science AG, D-51368 Leverkusen, as shown in Fig. 9(a). The physical properties of TPU are summarized in Table 11. HNTs, in powder form with an average size of 20 nm, were purchased from Natural Nano, Inc., 832 Emerson Street, Rochester, New York, as shown in Fig. 9(b). The chemical composition of HNTs and the physical properties of HNTs are summarized in Tables 12 and 13, respectively. The melting temperature of TPU matrix is 200 °C as recommended by the manufacturer.

Instrumentation

Transmission Electron Microscopy (TEM), using a Philips CM12 Somerset, New Jersey, US), operated at 80 kV and producing an electron beam capable of interacting with the sample as it passes through, was used to provide images showing the existence of the nanotubes. TEM was used in many fields in science, engineering and medicine to examine the nanotube details at the surface. In this report, TEM was used to identify and locate the nanotubes and to measure the geometrical dimensions of their inner and outer diameters. In addition to TEM, a FESEM, model ZEISS SUPRA 55-VP (Manufacturer, Konigsallee, Deutschland) with a magnification up to 25.00 k×, was used to investigate and view small structures on the surface of the HNTs and HNTs-TPU nanocomposites. The FESEM was equipped with high resolution images and had insignif-

icant charging effects on the HNTs-TPU nanocomposites surface at a very high spatial resolution of about 1.50 nm, which was 3–6 times that of the TEM. The thermal properties of the HNTs-TPU nanocomposites were investigated using a Thermogravimetric analyser; model Q600, a product of TA Instruments, New Castle, US with heating rate of 10 °C per min. The mixture of the HNTs-TPU nanocomposites were performed with a Brabender mixer (Model W 50 EHT) Corder PL 2000 compounder equipped with a 50 cm^3 kneader chamber. For the preparation of specimens for testing, the injection apparatus DSM Xplore moulding injection machine was used. The heating chamber of 10 cm^3 can be heated up to 350 °C. To investigate tensile strength and strain, an Instron Universal Testing Machine (INSTRON 5567) was used.

Preparation of the injection moulding specimens

The drying process of the HNTs and TPU matrix were carried out in an oven at a temperature of 80 °C for 12 h [15]. Following drying, the HNTs-TPU nanocomposites were homogenized using a Brabender mixer [47,48]. The matrix was mixed until stabilization of the torque and was followed by adding filler into the mixer. The mixture was then injected using a moulding machine, whereby four samples were produced including the neat sample, as shown in Fig. 10(a)–(d) at loading percentages of 0 (TPU matrix), 1, 2 and 3 wt.% HNTs, respectively. The dimensions of the samples are shown in Fig. 10(e).

Conclusion

Despite the fact that the technology of the HNTs-TPU nanocomposites is very advancing technology, many technical challenges such as the preparation of the samples are still important and they need to undergo some regulations. One of these challenges is the sensitivity of the results due to the methods of sample preparations. To reduce the significant of the technical challenges, Taguchi method of optimization and ANOVA were used in this article. The main topic of analysis was performed by considering the absolute variation of the mechanical properties (tensile strength, Young's modulus, and tensile strain) in accordance with the effect of wt.% HNTs loading to TPU. It was found that absolute variation between the highest and lowest tensile strength (69%) is purely attributed to only three controlled parameters (mixing temperature, mixing speed, and HNTs loading) while the mixing time shows no effect. The support for this result comes from ANOVA analysis, FESEM images, and DSC results. The results suggests that 1 wt.% HNTs loading to TPU processed at temperature of 190 °C and mixing speed of 30 rpm are enough to produce the optimized HNTs-TPU nanocomposites. The outcome of this result could have important effect on the cost and the future of the nanocomposites.

Table A1
The parameters for three levels of selected factors.

Factors	Level 1	Level 2	Level 3
Mixing temp. (°C)	190	200	210
Mixing speed (rpm)	30	40	50
Mixing time (min)	20	30	40
HNTs loading (wt.%)	1	2	3

Acknowledgments

The authors thank Universiti Kebangsaan Malaysia and the Ministry of Higher Education Malaysia for the financial support grant DIP-2014-006 and LRGS/TD/2012/USM-UKM/PT/05.

Appendix A

Step 1: Selection of factors using Taguchi design:
Four factors were chosen at three levels each, as shown in Table A1, and nine experiments were chosen using Taguchi design.

Step 2: The combination of parameters on the orthogonal L_9 (3^4) array

Each of the nine experiments was run at four factors as proposed by the Taguchi design. The data in Table 2 show the optimizing factors of tensile strength, Young's modulus, and tensile strain, classified and arranged by Mintab.

Step 3: Calculation of the average of each response (tensile strength, Young's modulus, and tensile strain)

In order to calculate the average tensile strength, Young's modulus and tensile strain, nine experiments were run at optimizing parameters, which resulted in nine runs. Each run was divided into three specimens and each specimen was tested for each of the three responses and finally the average value was calculated, as shown in Table A2 for tensile strength; Table A3 for Young's modulus; and Table A4 for tensile strain.

Step 4: Calculation of S/N

This step was to determine the S/N ratio for each response of the tensile strength, Young's modulus, and tensile strain. First, the mean-square deviation (MSD) was calculated according to Eq. (A1):

$$MSD = \frac{\sum_{i=1}^{n} \frac{1}{y_i^2}}{n} \quad (A1)$$

where y_i the value of tensile strength for the ith test is; n is the number of tests. An example of calculating MSD is shown as follows:

$$\text{MSD} = \frac{\left(\frac{1}{25.493^2}\right) + \left(\frac{1}{24.886^2}\right) + \left(\frac{1}{25.381^2}\right)}{3} = 0.0015685$$

Table A2
Calculation of the average of tensile strength.

No. run	Mixing temp.	Mixing speed	Mixing time	HNTs loading	Rep 1	Rep 2	Rep 3	Average
1	190	30	20	1	25.49	24.88	25.38	25.25
2	190	40	30	2	16.78	22.93	17.80	19.17
3	190	50	40	3	16.89	15.66	14.82	15.79
4	200	30	30	3	16.85	16.37	17.16	16.79
5	200	40	40	1	19.63	18.90	18.63	19.05
6	200	50	20	2	17.54	17.39	17.70	17.54
7	210	30	40	2	21.36	20.57	21.80	21.24
8	210	40	20	3	13.85	12.18	13.36	13.13
9	210	50	30	1	20.74	20.34	22.33	21.13

Table A3
Calculation of the average of Young's modulus.

No. run	Mixing temp.	Mixing speed	Mixing time	HNT loading	Rep 1	Rep 2	Rep 3	Average
1	190	30	20	1	2.40	5.00	2.96	3.45
2	190	40	30	2	8.46	3.92	7.23	6.54
3	190	50	40	3	10.71	11.33	9.55	10.53
4	200	30	30	3	9.68	10.41	10.26	10.12
5	200	40	40	1	8.58	7.28	7.46	7.77
6	200	50	20	2	7.60	8.17	8.39	8.05
7	210	30	40	2	5.36	6.87	5.92	6.05
8	210	40	20	3	11.30	11.42	11.90	11.54
9	210	50	30	1	6.62	5.89	4.38	5.63

Table A4
Calculation of the average of tensile strain.

No. run	Mixing temp.	Mixing speed	Mixing time	HNT loading	Rep 1	Rep 2	Rep 3	Average
1	190	30	20	1	997.1	1054.0	1101.0	1050.7
2	190	40	30	2	989.5	971.9	1010.0	990.4
3	190	50	40	3	590.5	615.7	618.4	608.2
4	200	30	30	3	682.4	672.3	687.6	680.7
5	200	40	40	1	1029.5	1008.0	1009.0	1015.5
6	200	50	20	2	890.4	843.3	876.7	870.1
7	210	30	40	2	1004.2	994.6	1019.0	1005.9
8	210	40	20	3	506.8	499.4	519.7	508.6
9	210	50	30	1	1056.4	1046.0	989.1	1030.5

Finally, the S/N ratios were calculated according to Eq. (A2):

$$S/N_{LB} = -10\log(MSD) \quad (A2)$$

As an example of an S/N ratio:

$$S/N_{LB} = -10\log(MSD) = 28.0464$$

The average of the responses of the tensile strength, Young's modulus, and the tensile strain and their relevant S/N ratios are collectively shown in Table 3.

References

[1] Gaaz TS et al. Properties and applications of polyvinyl alcohol, halloysite nanotubes and their nanocomposites. Molecules 2015;20(12):22833–47.
[2] Cavallaro G et al. Films of halloysite nanotubes sandwiched between two layers of biopolymer: from the morphology to the dielectric, thermal, transparency, and wettability properties. J Phys Chem C 2011;115 (42):20491–8.
[3] Liu M et al. Recent advance in research on halloysite nanotubes-polymer nanocomposite. Prog Polym Sci 2014;39(8):1498–525.
[4] Dong Y et al. Multi-response analysis in the material characterisation of electrospun poly (lactic acid)/halloysite nanotube composite fibres based on Taguchi design of experiments: fibre diameter, non-intercalation and nucleation effects. Appl Phys A 2013;112(3):747–57.
[5] Cordeiroa S, Marques M. Natural nanotubes reinforcing heterophasic polypropylene. Mater Res 2015;18(2):267–73.
[6] Mittal V. Characterization techniques for polymer nanocomposites. John Wiley & Sons; 2012.
[7] Szpilska K, Czaja K, Kudła S. Halloysite nanotubes as polyolefin fillers. Polimery 2015;60(6):359–71.
[8] Pasbakhsh P, Churchman GJ, Keeling JL. Characterisation of properties of various halloysites relevant to their use as nanotubes and microfibre fillers. Appl Clay Sci 2013;74:47–57.
[9] Gaaz TS et al. Optimizing injection molding parameters of different halloysites type-reinforced thermoplastic polyurethane nanocomposites via Taguchi complemented with ANOVA. Materials 2016;9:947–56.
[10] Rajan KP et al. Optimization of processing parameters for a polymer blend using Taguchi method. Yanbu J Eng Sci 2010;1:59–67.
[11] Finnigan B et al. Morphology and properties of thermoplastic polyurethane nanocomposites incorporating hydrophilic layered silicates. Polymer 2004;45 (7):2249–60.
[12] Gholami M, Mir Mohamad Sadeghi G. Investigating the effects of chemical modification of clay nanoparticles on thermal degradation and mechanical properties of TPU/nanoclay composites. J Particle Sci Technol 2015;1(1):1–11.
[13] Barick AK, Tripathy DK. Effect of organically modified layered silicate nanoclay on the dynamic viscoelastic properties of thermoplastic polyurethane nanocomposites. Appl Clay Sci 2011;52:312–21.
[14] You KM, Park SS, Lee CS, Kim JM, Park GP, Kim WN. Preparation and characterization of conductive carbon nanotube-polyurethane foam composites. J Mater Sci 2011;46:6850–5.
[15] Bian J et al. Fabrication of microwave exfoliated graphite oxide reinforced thermoplastic polyurethane nanocomposites: effects of filler on morphology, mechanical, thermal and conductive properties. Compos A Appl Sci Manuf 2013;47:72–82.
[16] Pang JS et al. Taguchi design optimization of machining parameters on the CNC end milling process of halloysite nanotube with aluminium reinforced epoxy matrix (HNT/Al/Ep) hybrid composite. HBRC J 2014;10(2):138–44.
[17] Joussein E et al. Halloysite clay minerals—a review. Clay Miner 2005;40 (4):383–426.
[18] Harvey CC, Murray HH. Geology, mineralogy and exploitation of halloysite clays of Northland, New Zealand. Clay Miner Soc Spec Pub 1990;1:233–48.
[19] Jia Z et al. Morphology, interfacial interaction and properties of styrene-butadiene rubber/modified halloysite nanotube nanocomposites. Chin J Polym Sci 2009;27(06):857–64.
[20] Davim JP. Statistical and computational techniques in manufacturing. Springer Science & Business Media; 2012.
[21] Shokoohi S, Arefazar A, Naderi G. Compatibilized polypropylene/ethylene–propylene–diene-monomer/polyamide6 ternary blends: effect of twin screw extruder processing parameters. Mater Des 2011;32(3):1697–703.
[22] Prashantha K et al. Taguchi analysis of shrinkage and warpage of injection-moulded polypropylene/multiwall carbon nanotubes nanocomposites. Exp Polym Lett 2009;3(10):630–8.
[23] Rafizadeh M et al. Experimental relationship for impact strength of PC/ABS blend based on the Taguchi method. Iran Polym J 2005;14(10):881–9.
[24] Kenett R, Zacks S, Amberti D. Modern industrial statistics: with applications in R, MINITAB and JMP. John Wiley & Sons; 2013.
[25] Huang HX, Deng ZW. Effects and optimization of processing parameters in water-assisted injection molding. J Appl Polym Sci 2008;108(1):228–35.
[26] El-Shekeil YA et al. Optimization of blending parameters and fiber size of kenaf-bast-fiber-reinforced the thermoplastic polyurethane composites by Taguchi method. Adv Mater Sci Eng 2013;2013.
[27] Lai C et al. Mechanical and electrical properties of coconut coir fiber-reinforced polypropylene composites. Polym-Plast Technol Eng 2005;44(4):619–32.
[28] Yang R, Mather R, Fotheringham A. The application of factorial experimental design to the processing of polypropylene fibres. J Mater Sci 2001;36 (13):3097–101.
[29] Ghalme S, Mankar A, Bhalerao YJ. Parameter optimization in milling of glass fiber reinforced plastic (GFRP) using DOE-Taguchi method. SpringerPlus 2016;5:1376–85.
[30] Liu J, Lu P, Weng W. Studies on modifications of ITO surfaces in OLED devices by Taguchi methods. Mater Sci Eng B 2001;85(2):209–11.
[31] Mehat NM, Kamaruddin S. Optimization of mechanical properties of recycled plastic products via optimal processing parameters using the Taguchi method. J Mater Process Technol 2011;211(12):1989–94.
[32] Azaman M et al. Optimization and numerical simulation analysis for molded thin-walled parts fabricated using wood-filled polypropylene composites via plastic injection molding. Polym Eng Sci 2015;55(5):1082–95.
[33] Wang X, Zhao G, Wang G. Research on the reduction of sink mark and warpage of the molded part in rapid heat cycle molding process. Mater Des 2013;47:779–92.

[34] Hakimian E, Sulong AB. Analysis of warpage and shrinkage properties of injection-molded micro gears polymer composites using numerical simulations assisted by the Taguchi method. Mater Des 2012;42:62–71.
[35] Asiltürk I, Akkus H. Determining the effect of cutting parameters on surface roughness in hard turning using the Taguchi method. Measurement 2011;44 (9):1697–704.
[36] Nasir S et al. Comparison between single and multi gates for minimization of warpage using Taguchi method in injection molding process for ABS material. In: Key engineering materials. Trans Tech Publ.; 2014.
[37] Nayani M, Gunashekar S, Abu-Zahra N. Synthesis and characterization of polyurethane-nanoclay composites. Int J Polym Sci 2013;2013.
[38] Barick AK, Tripathy DK. Preparation, characterization and properties of acid functionalized multi-walled carbon nanotube reinforced thermoplastic polyurethane nanocomposites. Mater Sci Eng B 2011;176(18):1435–47.
[39] Osman AF et al. Structure–property relationships in biomedical thermoplastic polyurethane nanocomposites. Macromolecules 2011;45(1):198–210.
[40] Barick AK, Tripathy DK. Effect of organoclay on thermal and dynamic mechanical properties of novel thermoplastic polyurethane nanocomposites prepared by melt intercalation technique. Polym Adv Technol 2010;21 (12):835–47.
[41] Russo P et al. Tensile properties, thermal and morphological analysis of thermoplastic polyurethane films reinforced with multiwalled carbon nanotubes. Eur Polym J 2013;49(10):3155–64.
[42] El-Shekeil Y et al. Influence of chemical treatment on the tensile properties of kenaf fiber reinforced thermoplastic polyurethane composite. Exp Polym Lett 2012;6(12).
[43] Barick AK, Tripathy DK. Effect of nanofiber on material properties of vapor-grown carbon nanofiber reinforced thermoplastic polyurethane (TPU/CNF) nanocomposites prepared by melt compounding. Compos A Appl Sci Manuf 2010;41(10):1471–82.
[44] Bhuvana S, Prabakaran M. Synthesis and characterisation of polyamide/halloysite nanocomposites prepared by solution intercalation method. Nanosci Nanotechnol 2014;4(3):44–51.
[45] Marini J et al. Elaboration and properties of novel biobased nanocomposites with halloysite nanotubes and thermoplastic polyurethane from dimerized fatty acids. Polymer 2014;55(20):5226–34.
[46] Goh PS et al. Recent advances of inorganic fillers in mixed matrix membrane for gas separation. Sep Purif Technol 2011;81(3):243–64.
[47] Toldy A et al. Flame retardancy of thermoplastics polyurethanes. Polym Degrad Stab 2012;97(12):2524–30.
[48] Sureshkumar M et al. Optimization of process parameters of immiscible blends of linear low-density polyethylene and poly dimethyl siloxane rubber using Taguchi methodology. Polym-Plast Technol Eng 2008;47(4):341–5.